The plume spreading in the MADE transport experiment: Could it be predicted by stochastic models?

A. Fiori,[1] G. Dagan,[2] I. Jankovic,[3] and A. Zarlenga[1]

Received 29 June 2012; revised 11 January 2013; accepted 5 February 2013.

[1] The transport experiment at the MADE site (a highly heterogeneous aquifer) was investigated extensively in the last 25 years. The longitudinal mass distribution $m(x,t)$ of the observed solute plume differed from the Gaussian shape and displayed strong asymmetry. This is in variance with the prediction of stochastic models of flow and transport in weakly heterogeneous aquifers. In the last decade, we have forwarded a model coined as MIM (multi-indicator), in which the heterogeneous structure consists of blocks of different of different and independent random lognormal K. Thus, the structure is completely characterized by K_G (the geometric mean), σ_Y^2 (the logconducitvity variance) and the integral scale I. Flow (uniform in the mean) and advective transport were solved by the semianalytical SCA (self-consistent approximation). The SCA models the travel time of a solute parcel from an injection to a control plane as a sequence of independent time steps, each resulting from the simple solution for isolated blocks surrounded by a uniform matrix. The aim of the article is to determine whether the model could predict the observed mass distribution of MADE ($\sigma_Y^2 \simeq 7$ based on the most recent direct-push injection logger data), by using the recently collected detailed K data and the observed mean head gradient. It was found that the agreement with the measured plume is quite satisfactory, differences related to incomplete mass recovery, injection condition and ergodicity notwithstanding. It is concluded that the physical mechanism of advection, modeled by the local ADE, and the heterogeneity of K, are able to explain the MADE plume behavior and the stochastic model could predict it.

Citation: Fiori, A., G. Dagan, I. Jankovic, and A. Zarlenga (2013), The plume spreading in the MADE transport experiment: Could it be predicted by stochastic models? *Water Resour. Res.*, *49*, doi:10.1002/wrcr.20128.

1. Introduction and Background

[2] Modeling transport of solutes in aquifers is a central topic of subsurface hydrology. For the sake of completeness and for clarification of nomenclature, we shall describe briefly the developments which led to the stochastic approach and to the methodology of the present study.

[3] In its early development, the experimental investigation of transport in porous media was carried out at the laboratory scale by injecting a pulse of inert solute of concentration C_0 at the inlet of a column in which water flowed with Darcian velocity U. Measurement of the concentration C at the outlet revealed that C can be quantified by a Gaussian distribution, solution of the equation

$$\frac{\partial C}{\partial t} + U\frac{\partial C}{\partial x} = D_{dL}\frac{\partial^2 C}{\partial x^2}. \quad (1)$$

[4] The longitudinal pore-scale dispersion coefficient could be written as $D_{dL} = D_{dm} + \alpha_{dL}U$, where the Peclet number Pe_d is defined by $Pe_d = Ud/D_{dm}$, d is the pore size and D_{dm} is the effective molecular diffusion coefficient. Measurements showed that the pore-scale (hydrodynamic) dispersivity α_{dL} is O(d) and generally the mechanical dispersion term $\alpha_{dL}U \gg D_{dm}$ [see, e.g., *Bear*, 1988]. The transverse dispersivity α_{dT} was found to be smaller than α_{dL} by 1–2 orders of magnitude.

[5] Observation of plumes at the aquifer scale indicated that their longitudinal spreading is much larger than the one caused by pore-scale dispersion and the ad hoc approach [*Bear*, 1988] was to assume that (1) prevails, but with D_{dL} and α_{dL} replaced by the macrodispersion (field scale) and macrodispersivity coefficients D_L and α_L, respectively, where $\alpha_L \gg \alpha_{dL}$. This increase was attributed to the spatial variability (heterogeneity) of the hydraulic conductivity $K(\mathbf{x})$ and the related one of the Darcian velocity $\mathbf{V}(\mathbf{x}, t)$. The intuitive reasoning is that field scale spreading is caused by the velocity spatial variation, e.g., the contrast between the large ones prevailing in regions of high conductivity and the smaller ones in low K zones. Such an approach posed a few fundamental questions: how is spreading defined and what is the scale of definition of C? Is macrodispersivity constant? How can it be related to the conductivity spatial variability?

[1]Dipartimento di Ingegneria, Universita' di Roma Tre, Rome, Italy.
[2]School of Mechanical Engineering, Tel Aviv University, Ramat Aviv, Israel.
[3]Department of Civil, Structural and Environmental Engineering, State University of New York at Buffalo, Buffalo, USA.

Corresponding author: A. Fiori, Universita' di Roma Tre, via Volterra 62, Rome I-00146, Italy. (aldo@uniroma3.it)

0043-1397/13/10.1002/wrcr.20128

[6] To address these questions in a systematic and rational manner, the starting point is the usual steady flow

$$\mathbf{V}(\mathbf{x}) = -\frac{K(\mathbf{x})}{\theta}\nabla H, \nabla.\mathbf{V} = 0 \rightarrow \nabla^2 H + \nabla Y.\nabla H + \ (Y = \ln K), \tag{2}$$

and transport

$$\frac{\partial C}{\partial t} + \mathbf{V}.\nabla C + \nabla.(\mathbf{D}_{\mathrm{d}}\nabla C), \tag{3}$$

equations, where θ stands for porosity (assumed here to be constant), H is the head, C is the local concentration (e.g., as measured over a sample of decimetric scale centered at $\mathbf{x}$) of an inert solute and $\mathbf{D}_d$ is the pore-scale dispersion tensor. Equations (2) and (3), whose solutions are sought, are obeyed at each point of the aquifer. We shall denote (3) as LADE, the local advection dispersion equation; it is a 3-D extension of (1). In principle, the solution involves the following steps: to solve first the flow equation (2) for $H(\mathbf{x})$ in a domain Ω, with given $K(\mathbf{x})$ and appropriate boundary conditions on $\partial\Omega$, subsequently to derive $\mathbf{V}$, which serves as an input to (3) and finally to solve the transport equation (3), for given $\mathbf{D}_d$. This is a formidable task, which faces a few obstacles: (i) in most aquifers, and particularly in the highly heterogeneous ones of concern here, K varies in a seemingly erratic manner in space by orders of magnitude and field data are scarce; as a consequence K spatial distribution is subjected to uncertainty; (ii) solving numerically (2,3) for such K fields is extremely demanding in terms of computational resources, especially for the 3-D configurations considered here; (iii) in many applications the interest is in some global parameters of the solute plume, e.g., the breakthrough curve (BTC) at a control surface or a well; thus, solving first for the local C is superfluous, if the BTC can be determined directly.

[7] These difficulties have led to the emergence of the stochastic approach, which has known a tremendous development in the last 35 years [see e.g., the monographs by *Dagan*, 1989, *Gelhar*, 1993, *Rubin*, 2003]. Thus, Y (or K) is modeled as a random space function (RSF), and consequently all the flow and transport dependent variables in (2,3) are RSF as well, characterized statistically. To simplify matters, toward application to MADE, we adopt the following common assumptions: (i) Y is stationary of normal univariate pdf, of mean $\langle Y\rangle = \ln K_G$ and variance σ_Y^2, and of stationary axisymmetric autocorrelation $\rho_Y(r')$. Here $r' = [(r_x^2 + r_y^2)/I^2 + r_z^2/I_v^2]^{1/2}$, $\mathbf{r}$ is the lag vector, I and I_v are the horizontal and vertical integral scales, respectively, and $f = I_v/I < 1$ is the anisotropy ratio; (ii) the flow is uniform in the mean i.e., $\langle\nabla H\rangle = -\mathbf{J}, \langle\mathbf{V}\rangle = \mathbf{U} = K_{efh}\mathbf{J}/\theta$, where $\langle\rangle$ stands for ensemble mean, K_{efh} is the horizontal effective conductivity, $\mathbf{J}(J, 0, 0)$ and $\mathbf{U}(U, 0, 0)$ are constant and the velocity field is stationary in the region of interest (sufficiently far from boundaries); (iii) the inert solute plume of initial mass M_0 is injected instantaneously at $t = t_0$ in a volume V_0 or an area A_0 at $x = 0$, in a resident or flux proportional mode (the extension to continuous injection is straightforward); (iv) the plume is quantified by the BTC $M(x, t)/M_0$ where M is the mass of solute which has moved past a control plane (CP) at x, at time t. Of particular interest here are the associated relative mass flux $\mu = \partial(M/M_0)/\partial t$ or longitudinal relative mass distribution function $m(x,t) = -\partial(M/M_0)/\partial x = (1/M_0)\int\int C(x,y,z,t)\mathrm{d}y\mathrm{d}z$; (v) generally M, μ, or m are random, but we assume in this stage that the initial plume is large enough to ensure ergodicity, i.e., they are approximately equal to their ensemble means. Then, the restricted objective considered here is to determine $m(x,t)$ (or μ) for given statistical moments of $Y(\mathbf{x})$, given J and the above initial conditions for C. Under these circumstances, μ and m are equal to the pdf of travel time τ and solute particle longitudinal displacements X, respectively.

[8] This task is still a difficult one and approximations have been adopted in the past in order to simplify the solution. The most common one is the first-order solution of the flow and transport in σ_Y^2, applying to weakly heterogeneous formations (the approach and the various applications are described e.g., in *Dagan* [1989] and *Rubin* [2003]). In this case $m(x, t)$ obeys the Gaussian ADE (GADE)

$$\frac{\partial m}{\partial t} + U\frac{\partial m}{\partial x} = D_L(t - t_0)\frac{\partial^2 C}{\partial x^2}, \tag{4}$$

where D_L and $\alpha_L = D_L/U$ are the macrodispersion and macrodispersivity coefficients, respectively. They have been determined in an analytical form for isotropic aquifers or by a quadrature for anisotropic ones [see *Dagan*, 1989, Figure 4.6.4 for the apparent $\alpha_{Lap} = (1/t)\int_0^t D_L(t')\ \mathrm{d}t'$, or *Dagan et al.*, 2008, Figure 6 for α_L). An important observation is that the local dispersion term $\mathbf{D}_d$ in (3) has little impact on D_L for the usual high values of the Peclet number $Pe = UI/D_m$ [*Fiori*, 1996; *Berglund and Fiori*, 1997]. Thus, α_L was derived in the simplest version [e.g., *Dagan*, 1989] by using the local advection equation $\partial C/\partial t + \mathbf{V}(\mathbf{x}).\nabla C = 0$ as the starting point, in its Lagrangean version (known as particle tracking in the numerical context). The macrodispersivity was found to grow from zero at $t = t_0$ to a constant value during a "setting time" $t_s U/I \approx 10$, stabilizing at the common value $\alpha_L = \sigma_Y^2 I$. The dependence of α_L/I upon tU/I is quite insensitive to the value of anisotropy ratio f, a property which is valid for highly heterogeneous media as well [*Zarlenga et al.*, 2012b]. Thus, the simple analytical solution for $f = 1$ can be used with confidence for any f. The asymptotic value $\alpha_L = \sigma_Y^2 I$ was obtained by *Gelhar and Axness* [1983], from the Eulerian equation by a double expansion in σ_Y^2 and $tU/I \gg 1$. In line with the literature, we shall denote this limit of (4) as the Fickian ADE (FADE). Another important observation is that the structural information needed for solving (2,3) at first order is the two point covariance C_Y solely, which makes the approach quite robust. Indeed, this is the type of information which can be identified at best from field data, even for well-characterized aquifers. However, a complete statistical characterization of the Y random field requires knowledge of higher order and multipoint correlations, which are generally not achievable. To overcome this difficulty it is common in numerical simulations to adopt for Y a multi-Gaussian structure, i.e., the values of Y at an arbitrary set of points is a multivariate normal vector; then any moment can be expressed in terms of C_Y. This assumption should be

regarded as one of convenience rather than supported by data and we shall return to this important issue in the sequel. It is worthwhile to recall here the following relationships stemming from (4): $\int_0^\infty m\ \mathrm{d}x = 1, U = \mathrm{d}\overline{x}/\mathrm{d}t, D_L = (1/2)\mathrm{d}m_2/\mathrm{d}t$ where $\overline{x} = \int xm(x,t)\mathrm{d}x$ is the centroid and $m_2 = \int (x-\overline{x})^2 m(x,t)\mathrm{d}x$ is the plume second-longitudinal spatial moment. These relationships are usually employed in order to determine U and D_L from measurements or numerical simulations, even if m is not exactly Gaussian.

[9] Though (4) and (1) are mathematically similar, their meaning is profoundly different: (i) while C in (1,3) stands for the local concentration, m is a plume global parameter, resulting from the integration of C over the plume cross section; (ii) the macrodispersivity depends on the travel time and is therefore nonlocal and it stabilizes only after the setting time t_s or distance t_sU; (iii) the macrodispersivity depends on the heterogeneous aquifer structure. Still, it is common to regard (4) with α_L constant as the "classical ADE".

[10] A few elaborate field tests were conducted in the past in order to validate the stochastic approach. Thus, two well-documented ones were at Borden Site [*Mackay et al*., 1986; *Freyberg*, 1986; *Sudicky*, 1986] and Cape Cod [*LeBlanc et al*., 1991; *Garabedian et al*., 1991]. Both aquifers are weakly heterogeneous, with the field determined $\sigma_Y^2 = 0.36$ and $\sigma_Y^2 = 0.25$, respectively. Comprehensive discussions of these tests have been published in the past and the general conclusion was that the longitudinal spreading of the measured plumes as quantified by α_L was in fair agreement with the first-order results.

[11] However, many aquifers are highly heterogeneous ($\sigma_Y^2 > 1$) and the transport experiment, known as MADE [*Boggs et al*., 1992; *Boggs and Adam*, 1992; *Rehfeldt et al*., 1992; *Adams and Gelhar*, 1992; *Boggs et al*., 1993] was initiated and carried out at the Columbus Air Base in 1986 in order to investigate the applicability of the stochastic theory to an aquifer with $\sigma_Y^2 \simeq 7$. This field test has been the topic of a large number of publications covering all its aspects: geology, conductivity spatial variability, flow conditions, plume measurements, interpretation and modeling. The effort was summarized recently in an overview paper by *Zheng et al*. [2011] which includes a comprehensive bibliography. As far as the main features of transport are concerned, the measurements are encapsulated by the relative mass m spatial distributions at a few fixed times. The main finding of the experiment was that the measured plume differed markedly from those pertaining to the aforementioned weakly heterogeneous aquifers. More precisely, unlike the Gaussian distribution implied by (4), m is highly skewed and cannot be characterized by the first-spatial and second-spatial moments and the associated macrodispersivity. This finding has motivated derivation of transport models which attempt to represent the MADE observed plumes, two noteworthy ones being the CTRW [see e.g., *Berkowitz and Scher*, 1998] and the dual domain mass transfer model [*Harvey and Gorelick*, 2000; *Feehley et al*., 2000; *Guan et al*., 2008]. These models are not replacing the basic LADE (2,3), but they aim at overcoming the shortcomings of the first-order approximation (4) in modeling transport in highly heterogeneous formations. This point is made clear by the following paragraph of the review of *Zheng et al*. [2011, p. 655]: "... if microscale variations of water flux due to aquifer heterogeneity could be precisely described, the natural model would be based solely on a combination of advection and molecular diffusion...". A similar conclusion was drawn by *Salamon et al*. [2007] in their analysis of the MADE experiment. It is not our purpose to discuss here either the theoretical merits of the two aforementioned models or their ability to capture the behavior of the MADE observed plume. The point of interest here is that these models, unlike (4), contain parameters which are not always directly related to the conductivity statistics, but have to be determined from transport experiments. In our view this requirement limits their use as predictive tools, since carrying out transport experiments in order to characterize sites is costly and of prolonged duration, which is quite prohibitive in most applications.

[12] We have developed in the last decade (see section 3) an approximate stochastic model of flow and transport in highly heterogeneous formations which uses the LADE (3) as the starting point and requires as input the structural information about Y, similarly to the first-order approximation. We coined the model of the structure, consisting of an ensemble of blocks of independent K, as multi-indicator (MIM) and its properties are recalled in section 3 in the sequel. The resulting BTC, expressed in terms of $\mu(t, x)$ or the associated $m(x, t)$, indeed display the transition from the Gaussian to the skewed shape, as σ_Y^2 increases.

[13] The aim of the present study is to submit the model at the test of predicting the MADE plume development by using the head and hydraulic conductivity data collected at the site and to compare the outcome with the actual plume measurements.

[14] As for the K data, a large body was collected in the past by different methods. We base our analysis on the recent comprehensive coverage of the MADE field by [*Bohling et al*., 2012], who used the DPIL technology, as detailed in the following section. Based on the identified horizontal and vertical variograms, we concluded that the K spatial distribution can be modeled as a stationary random space function of univariate lognormal pdf and of stationary horizontal and vertical variograms, of finite sills and integral scales (see discussion below). The identified parameters K_G, σ_Y^2, I and I_v are sufficient for the application of MIM in its simplest mode, namely by assuming ergodicity and unconditional statistics. Thus, the procedure is underlain by an ensemble of a large number of independent realizations of the K field and the plume, which honor the data in a statistical sense. It is used to determine the unconditional mean $\langle m(x,t)\rangle$, which in turn is assumed to be close to the measured $m(x, t)$. From a theoretical standpoint, this is justified for plumes which cover a very large volume relative to the integral scale.

[15] A procedure which may relax the ergodicity requirements on one hand and even predict some local features of the plume on the other, is that of conditional statistics [see e.g., *Dagan*, 1989]. In principle it reduces the ensemble of realizations to a subensemble which honors actual K measurements at a few locations, particularly in the injection zone. This nonstationary approach is complex as it implies aggregation of data on one hand and adaptation of MIM on the other.

[16] The issues of the accuracy of the ergodicity assumption for the finite MADE plume and of conditioning are not

addressed by the present study which is an attempt to evaluate the predictive capability of the model in its simplest form.

[17] In view of the positive outcome and the relative simplicity of the model, we submit that it can provide a basis for transport prediction in highly heterogeneous aquifers.

[18] The plan of the paper is as follows: the relevant data of MADE are summarized in section 2, with a brief discussion of the problems encountered in the field; section 3 summarizes the MIM model and its extension to the MADE conditions; section 4 compares the predicted plume spreading by MIM with the measured one; and section 5 is devoted to conclusions. The Appendix describes the adaptation of the approximate transport model and the pertinent code used for prediction of MADE.

2. The MADE Field Data

[19] As mentioned above, MADE data collection and analysis were the topics of a few articles [see the recent review by *Zheng et al*., 2011]. Here we are going to summarize the information needed in order to apply the MIM model as a predictive tool and the plume data for comparison with prediction. We shall focus the analysis on the nonreactive tracers.

[20] We begin from the characterization of K, which was the object of a considerable effort invested in the last two decades. The recent paper by *Bohling et al*. [2012] summarizes the main results, which were obtained by two particular technologies (flowmeter and direct push). The recently developed direct-push injection logger (DPIL) technology uses a thin rod which is advanced by steps of 0.015 m downwards and water is injected through a screen at the tip. At each step the discharge and the pressure are measured. The latter serve to determine the local K at a support scale of 0.015 m [see e.g., *Liu et al*., 2010 for details about the various direct push methods], and *Bohling et al*. [2012] discuss the limitations of the methods. *Bohling et al*. [2012] showed that K is approximately lognormal and based on the derived horizontal and vertical variograms (Figure 6), we regarded $Y = \ln K$ as stationary. While the horizontal variogram has a sill (the common fluctuations at large lags notwithstanding), the vertical one displays a sill, followed by a sudden increase at lags larger than 6 m. Whether this is an observational effect (not seen in the flowmeter-based variogram) or an indication of nonstationarity, the effect on the modeling of the plume is practically immaterial since its vertical extent is around 7 m, as discussed in the sequel. At any rate, *Bohling et al*. [2012] present in their Tables 1 and 2 the estimates of the principal statistical parameters of K, and in particular the geometric mean K_G, the ln K variance σ_Y^2 and the horizontal and vertical integral scales I, I_v, respectively. Although the flowmeter and direct-push techniques led to somewhat similar results, the direct-push injection logger (DPIL) provided a much finer characterization of K, with a smaller support scale than the flowmeter, with an average K similar to that obtained by pumping tests. The parameters value obtained by the DPIL, which we adopt here are [*Bohling et al*., 2012]: $K_G = 8.9 \cdot 10^{-6}\,\mathrm{m/s}, \sigma_Y^2 = 6.6, I = 10.2\,\mathrm{m},\ I_v = 1.5\,\mathrm{m}$. The porosity data were analyzed by *Boggs et al*. [1992], who provided the mean value $\theta = 0.31$.

[21] The first transport experiment (hereinafter MADE-1) was conducted in years 1986–1988, and its results were reported in a few papers [e.g., *Boggs et al*., 1992; *Adams and Gelhar*, 1992]. A second experiment (MADE-2) was performed in 1990–1991 [*Boggs et al*., 1993]; the same injection/monitoring wells were used in both experiments, although the conservative tracers were different, chloride and tritium, respectively. The plume was injected in a row of five wells, in a plane orthogonal to the mean velocity, at 1 m spacing. Thus, both the lateral and vertical sizes of the injected plume were much smaller than the correspondent integral scales, making solute transport likely a nonergodic process. However, the early snapshots reveal that the MADE-1 plume underwent a significant expansion in all directions soon after the injection, especially in the vertical; for instance, Figure 8a of *Boggs et al*. [1992] shows that after 49 days the vertical size of the plume was around 7 m, i.e., $4.7I_v$, and stayed more or less constant during the experiment. There was also a significant downstream and upstream spreading of the plume at the early time, as visible in the mass distributions. Thus, the "initial" size of the plume might have been much larger than the one inferred from the wells' configuration, leading to a transport process closer to the ergodic conditions assumed here.

[22] Seasonal fluctuations of the water table were observed in both experiments. *Boggs et al*. [1992] estimated an average head gradient $J = 0.003$, although Figure 4b of *Boggs et al*. [1992] indicates a range of variation of about $J = 0.003 \div 0.0045$, with an apparent mean around $J \simeq 0.0035$. Similarly, head gradient oscillations during the MADE-2 experiments were reported by *Guan et al*. [2008, Figure 8], suggesting an average gradient over the entire period of the experiment of about $J \simeq 0.0036$, i.e., similar to that of MADE-1.

[23] The plume was monitored by a system of multilevel samplers, the density of which decreased with the distance from the injection location, say after roughly 20 m from the injection wells, as visible in Figure 6 of *Boggs et al*. [1992]. The concentration field was sampled at different time instances, during "snapshots" of the C measured by the multilevel samplers. The mass distribution, integrated over a plane transverse to mean flow, was provided for six different snapshots in Figure 7 of *Adams and Gelhar* [1992] for MADE-1. We could not find the same quantity for MADE-2 in previous publications, except the experimental snapshot at time $t = 320$ days given by *Harvey and Gorelick* [2000]. The various snapshots are reproduced in Figures 2 in the sequel.

[24] Both experiments had problems with the plume mass recovery. In MADE-1, it varied from 200% at the first sampling round at $t = 49$ days, to 43% for the last one at $t = 503$ days. Similar trends were found for MADE-2, although the rate of recovery was higher for that experiment [*Harvey and Gorelick*, 2000]. *Adams and Gelhar* [1992] provided some possible explanation for the incomplete mass recovery, like e.g., cross talk between the sampling ports, horizontal/vertical plume truncations, horizontal resolution of the samplers and sampling bias. The latter implies that part of the mass is not sampled because it was "trapped" in the low-velocity regions which are present for high heterogeneity. This argument motivated in the recent years the use of mobile-immobile, mass transfer, models for

highly heterogeneous formations, like the MADE site (a comprehensive discussion is provided in the recent paper by *Zheng et al*. [2011]). It should be noted, however, that similar recovery rates were found for the Borden experiment [*Rajaram and Gelhar*, 1991], which is a weakly heterogeneous formation ($\sigma_Y^2 = 0.36$). Also, we remark that in highly heterogeneous formations the plume typically develops "fingers" or preferential channels, which may not be detected by some multilevel samplers (see also the discussion in *Adams and Gelhar* [1992]).

[25] The issue of whether the imperfect observed mass recovery is due to the limitations of the sampling procedure or an underlying physical mechanism, as implied by mass transfer models, is a matter of debate. It is emphasized that the application of MIM advective model is underlain by two considerations: (i) in the predictive mode addressed here the only available data are the K measurements and (ii) one of the distinctive feature of MIM is its modeling of high heterogeneity by accounting for the solute large residence time in elements of low permeability, which is similar to the immobile zone concept. However, our model does not require any additional structural parameter to account for the retention in the low K blocks.

3. The MIM Structural Model and Approximate Solution of Flow and Transport: Application to MADE

[26] As mentioned in the Introduction, we have advanced in the last decade the MIM permeability structural model and have solved the 3-D flow and transport equations with its aid. The adopted model was of an ensemble of spherical or spheroidal inclusions of different permeabilities, densely packed within a matrix of $K = K_{ef}$. Accurate solutions were derived numerically by elaborate codes, requiring considerable computer resources. The simulations served as numerical experiments which helped to elucidate the flow and transport mechanisms in highly heterogeneous media and to derive and validate simple approximate solutions. The latter are the ones of promise for prediction, and application to MADE is the object of the present study.

[27] It is worthwhile to mention two important findings: (i) the influence of local diffusion is negligible for the value of $Pe = UI_v/D_{dm} = 1000$ pertinent to MADE and advection is the only mechanism to be considered [*Janković et al*., 2009] and (ii) similarly to the first-order approximation the value of the anisotropy ratio $f = I_v/I$ has a minor impact upon the BTC and transport can be modeled by the simpler solution for isotropic media $f = 1$ (the issue is extensively analyzed in *Zarlenga et al*. [2012b]). This important result allows us to model the MADE plume by using the identified horizontal integral scale I only, which in turn was determined by *Bohling et al*. [2012] from the seemingly stationary horizontal variogram.

[28] Recently, we have extended the approach [*Fiori et al*., 2007; *Janković et al*., 2013] to the structure of cubes that tessellate continuously the space, which we shall employ for application to MADE. Herein, a succinct recapitulation of the MIM structure and the procedure to solve flow and transport.

[29] The formation is up made up from M adjacent cubical blocks of side $2R$, filling continuously a column Ω of length L and square cross section A, such that $\Omega = AL = 8R^3M$. The blocks are of constant, but different $K^{(i)}(i = 1,2, \ldots M)$. We denote by $\omega^{(i)}$ the volume of a block of conductivity $K^{(i)}$ and of centroid location $\overline{\mathbf{x}}^{(i)}(i = 1, 2, ..., M)$. Hence, the conductivity or logconductivity fields are given by

$$K(\mathbf{x}) = \sum_{i=1}^{M} K^{(i)} I\left(\mathbf{x} - \overline{\mathbf{x}}^{(i)}\right); \quad Y(\mathbf{x}) = \sum_{i=1}^{M} Y^{(i)} I\left(\mathbf{x} - \overline{\mathbf{x}}^{(i)}\right), \quad (5)$$

where the indicator function $I\left(\mathbf{x} - \overline{\mathbf{x}}^{(i)}\right) = 1$ for $\mathbf{x} \in \omega^{(i)}$ and $I\left(\mathbf{x} - \overline{\mathbf{x}}^{(i)}\right) = 0$ for $\mathbf{x} \notin \omega^{(i)}$. Due to the form of (5), the structure was coined as MIM, the multi-indicator model. The centers $\overline{\mathbf{x}}^{(i)}$ are located on a rectangular grid with nodes at equal distances in the x,y,z directions. The selected structure is defined by stating that $Y^{(i)}$ is a random normal vector and that $Y^{(i)}$ and $Y^{(k)}$ are uncorrelated for any $i \neq k$, i.e., permeabilities of inclusions are independent. Similarly $\overline{\mathbf{x}}^{(i)}$ are modeled as random variables to reflect the random shift among layers of elements in the horizontal planes as illustrated schematically in Figure 1a and accounted for in Appendix A. For the sake of generality, Figure 1a illustrates a medium of anisotropic structure; however, anistropy will be accounted in the derivation of the effective conductivity only, while it is immaterial for modeling of transport, which is based on cubical elements. For simplicity we refer to such isotropic structures in the following.

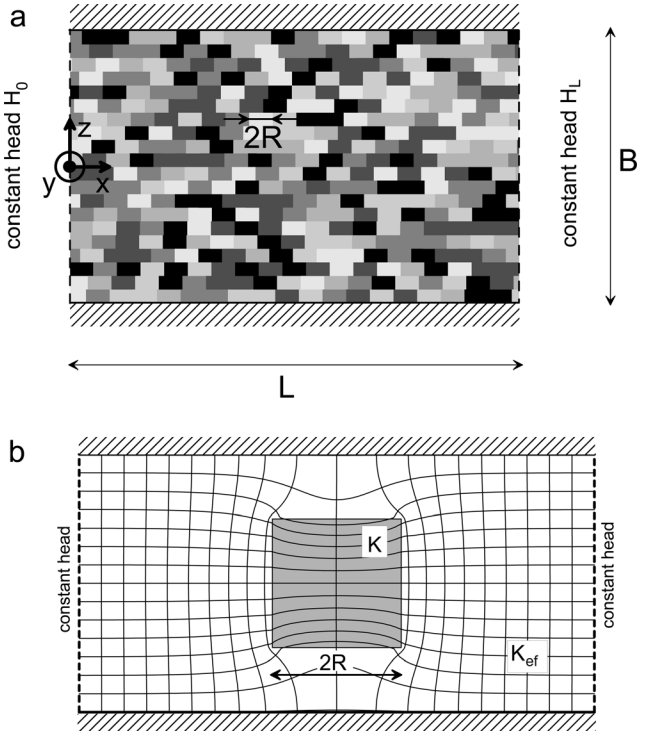

Figure 1. (a) Multi-indicator model for cuboid inclusions and (b) cross section through a symmetry plane showing flow net for a single highly conductive cube.

[30] The various multipoint covariances can de determined from (5). Thus, the two-point autocorrelation ρ_Y [e.g., section 1.9 of *Dagan*, 1989] is given by the product of linear functions

$$\rho_Y(\mathbf{r}) = \left(1 - \frac{r_x}{2R}\right)\left(1 - \frac{r_y}{2R}\right)\left(1 - \frac{r_z}{2R}\right) \text{ for } 0 < \mathrm{r_x}, \mathrm{r_y}, \mathrm{r_z} < 2\mathrm{R}\,;$$
$$\rho_Y(\mathbf{r}) = 0 \text{ otherwise}, \tag{6}$$

where $\mathbf{r}$ is the lag vector. The integral scale I of the isotropic structure is given by

$$\begin{aligned} I &= \int_0^\infty \rho_Y(r_x, 0, 0)\ \mathrm{d}r_x \\ &= \int_0^\infty \rho_Y(0, r_y, 0)\ \mathrm{d}r_y \\ &= \int_0^\infty \rho_Y(0, 0, r_z)\ \mathrm{d}r_z = R. \end{aligned} \tag{7}$$

[31] The MIM structure is different from the multi-Gaussian of same C_Y, and the difference manifests in higher order moments. For instance, the MIM has same correlation scales for any class of Y values. However, as mentioned already, field data are too scarce to allow for identifying moments higher than C_Y and in absence of additional information we regard (5) as a legitimate model of isotropic formations of lognormal univariate conductivity and finite integral scales.

[32] The solution of the flow problem consists in solving Laplace equation for the head H in each block, with continuity of H and normal velocity component at interfaces, and appropriate boundary conditions at the column boundary (constant heads at $x = 0$ and $x = L$, no flow on the lateral boundary, Figure 1a). Once the problem is solved, the space mean velocity is determined from $\overline{U} = (1/\Omega)\int_\Omega V_x(\mathbf{x})d\mathbf{x} = Q/(\theta A)$, where Q is the total discharge. Generally, $\overline{U}$ is random, but under the ergodic conditions achieved for sufficiently large $M \gg 1$, it tends to its ensemble mean value $U = \langle V_x \rangle$ and then the effective conductivity of the medium is defined by $K_{ef} = U/J = Q/(\theta JA)$.

[33] Advective transport is modeled by injecting a total mass of solute M_0, distributed over an area A_0, in the injection plane at $x = x_0$, within the core of stationarity of the flow domain Ω (Figure 1a). In the flux proportional injection mode [*Janković and Fiori*, 2010], the areal mass density is $m_0(y_0, z_0) = (M_0/A_0)V_x(y_0, z_0)/U$, where y_0, z_0 are coordinates in A_0. In the particle tracking approach, adopted in the numerical simulations, a large number of particles of mass $\Delta m_0 = m_0\ \Delta A_0$ are injected simultaneously at $t = 0$ and advected along the streamlines of the velocity field $\mathbf{V}(\mathbf{x})$, which was determined in the preceding step. Finally, the BTC at any control plane at $x > x_0$ is determined by the mass of particles which have moved beyond x at time t and the associated relative mass flux $\mu(x, t)$ by its time differentiation.

[34] These sequence of steps was used in our numerical investigation of flow and transport in MIM structures of spheres (for isotropic media) [*Janković et al*., 2003, 2006] and spheroids for anisotropic ones [*Suribhatla et al*., 2011; *Zarlenga et al*., 2012a] for high values of σ_Y^2. We have carried out new numerical simulations for cubical elements as well for $\sigma_Y^2 \leq 6$ by using an accurate finite differences code [*Janković et al.*, 2013] while transport was simulated by particle tracking. We have checked the ergodicity of results, which is obeyed due to the large size of the domain and initial plume and therefore regard them as ensemble averages as well. These simulations have validated the accuracy of the self consistent approximation (SCA), to be discussed next. For the sake of easiness, we recapitulate succinctly the relevant various steps of *Fiori et al*. [2007].

[35] The basic assumption of the SCA is that rather than solving the equations for the ensemble of blocks (Figure 1a), it is possible to solve for an isolated block of arbitrary conductivity K, submerged in a homogeneous matrix of the effective conductivity K_{ef} (Figure 1b). This is a much simpler problem and once the velocity field $\mathbf{V}(\mathbf{x}, K/K_{ef}) = \mathbf{U} + \mathbf{u}(\mathbf{x}, K/K_0)$ is determined, the approximate solution for the ensemble of blocks is given by $\mathbf{V}(\mathbf{x}) = \mathbf{U} + \int \mathbf{u}(\mathbf{x}, K/K_{ef})f(K)\mathrm{d}K$, where $f(K)$ is the pdf of K. The effective conductivity $K_0 = K_{ef}$ is determined from the self consistent argument, namely that $\mathbf{V} = \mathbf{U}$ leading to the integral equation $\int \mathbf{u}(\mathbf{x}, K/K_{ef})f(K)\mathrm{d}K = 0$. In the case of spheres, it becomes

$$\int_{-\infty}^{\infty} \frac{K/K_{ef} - 1}{2 + K/K_{ef}} f(Y')\mathrm{d}Y' = 0, Y = \ln(K/K_G), Y = \mathrm{N}\left[0, \sigma_Y^2\right], \tag{8}$$

which was apparently applied first time to K lognormal by *Dagan* [1979], to yield by a simple numerical iterative procedure the dependence of K_{ef}/K_G upon σ_Y^2. The result was found to be in excellent agreement with the full numerical solution for an ensemble of densely packed, nonlinearly interacting, inclusions for σ_Y^2 as large as 10 [*Janković et al*., 2003, Figure 3]. It also agrees with the numerical solution for cubes for $\sigma_Y^2 < 6$ [*Janković et al.,* 2013] and can be adopted for the latter. The intuitive reasoning underlying the SCA is that each cube is surrounded by a layer of 26 neighboring blocks which in the average can be replaced by a homogeneous medium of effective property.

[36] We have extended the approach in the past for transport [*Dagan et al*., 2003; *Fiori et al*., 2003; *Janković et al*., 2003; *Fiori et al*., 2006; *Janković et al*. 2006] along *Eames and Bush* [1999]. We have considered the isolated block of conductivity K submerged in the homogeneous matrix of K_{ef} and the associated velocity field $\mathbf{V}(\mathbf{x}') = \mathbf{U} + \mathbf{u}(\mathbf{x}')$, with the coordinates origin at the block center (Figure 1b). A thin planar plume is injected at $x' = -L$ upstream at time $t = 0$ and is advected past the block; after traveling over a sufficiently long distance L downstream, the distorted plume translates with velocity U, without changing anymore its shape. With the travel time given by $\tau = 2L/U + \tau_R$, the residual τ_R along any streamline for $-L < x' < L$ is obtained by a quadrature. We have found, along the solution for spheres, that the distribution of τ_R for $L \gg R$ can be approximated as follows: (i) τ_R is different from zero in the wake determined by the streamlines which cross the block and is very small outside; (ii) the area of the wake A_w is derived from $A_w/A_{in} = V_{in}/U = (2 + \kappa)/(3\kappa)$, where $A_{in} = 4R^2$ is

the cross-sectional area of the cube and V_{in} is the average velocity; (iii) the constant τ_R is equal to τ_M, the travel time along the central streamline of a sphere. The analytical expressions of $U\tau_M/R$ as function of κ are given by equations (A3)–(A4) of *Fiori et al*. [2007], and reproduced in the Appendix. It is represented in Figure A2 of *Fiori et al*. [2007], displaying excellent agreement with the numerically determined value. It is worthwhile to recall the asymmetric feature of τ_M: it is positive and tends to infinity like $4/(3\kappa)$ for $\kappa \to 0$, being determined almost exclusively by the delay within the low conductivity block; in contrast, it tends to a negative $U\tau_M/R$ finite value for $\kappa \to \infty$. This behavior has an essential role in explaining the skewness of plumes in highly heterogeneous media. In contrast, for weakly heterogeneous formations, τ_M at first order in $\ln \kappa$ is symmetrical [Figure A2 of *Fiori et al*., 2007].

[37] The procedure applied in the past to solve transport by the SCA was to assume that a large, ergodic, plume is injected at $x = 0$ and the mass flux $\mu(x, t)$ is computed at a control plane at a distance x, equal to a number N of blocks. Due to the ergodic hypothesis, i.e., the large number of blocks of independent K encountered by the plume, it experiences the entire spectrum of K values. Thus, the pdf $f(\tau_R)$ for the first layer, i.e., $x = \ell_1 = 2R$, is obtained by projecting the lognormal $f(\kappa)$ upon that of τ_R and weighing the latter by V_{in}/U, to account for the fact that the portion of the plume captured by a block of conductivity κ is proportional to the wake area. The dependence of $Rf(\tau_R, x)/U$ (for $x = 2R$) upon $\tau_R U/R$ is illustrated for $\sigma_Y^2 = 2$ in Figure 3 of *Fiori et al*. [2007], and indeed it is seen that $f(\tau_R)$ is skewed. The parameter σ_Y^2 impacts the result indirectly through the value of K_{ef} (8) and directly through $f(\kappa)$. For a plume moving past N layers the pdf $f(\tau_R, x)$ (for $x = 2NR$), identical to the mass flux μ, was obtained by the N-fold convolution of the Fourier Transform of $f(\tau_R, 2R)$. The expression for $f(\tau_R)$ is reproduced in *Fiori et al*. [2006; equation (12)], and its behavior for different σ_Y^2, including values close to that pertaining to MADE, is shown in Figure 2 of the same paper. Application to spherical and spheroidal inclusions for different x and σ_Y^2 displayed excellent agreement with numerical simulations for isotropic and anisotropic formations [*Zarlenga et al*., 2012a]. Hence, we can apply with confidence the SCA for cubes to MADE.

[38] It is worthwhile to mention that the SCA model was also successfully tested for structures different from the MIM one previously described, for instance against the accurate, finite-difference 2-D numerical simulation by *de Dreuzy et al*. [2007] and recent laboratory experiments of transport on a sandstone slab [*Major et al*., 2011; *Fiori et al*., 2012]. Also, SCA was evaluated against other available methods by *Frippiat and Holeyman* [2008], who found that SCA "produces close estimates of macrodispersivity" for high σ_Y^2, concluding that such model "could provide an important alternative to first-order stochastic theories". Thus, we gained enough confidence regarding the SCA capability to capture the features of flow and transport in highly heterogeneous formations.

[39] The application to MADE followed a somewhat different computational procedure than the one described above, due to the fact that the plume was quantified by the mass distribution $m(x, t)$ rather than μ, and furthermore, most of the plume stayed within two integral scales from the injection plane $x = 0$, which generally makes the numerical convolution problematic. Hence, a procedure more efficient than the previous one was developed specifically for the MADE implementation, and its details are presented in the Appendix.

4. Prediction of MADE Plume Spreading and Comparison with Measurements

[40] The SCA model outlined (section 3 and Appendix) was applied to the prediction of the MADE plume. Along the discussion of section 2, the latter may not entirely fulfill the ergodic conditions required by SCA, and the injection condition is not identical to the one adopted in our model (instantaneous injection over a larger transverse plane). Still, due to the early expansion of the plume during injection (section 2), it is assumed that the impact of the differences is not significant at the considered transport times.

[41] The set of structural parameters was chosen according to the DPIL data [*Bohling et al*., 2012], while the flow data were inferred from the papers which analyzed the MADE experiments, as discussed in section 2. Table 1 summarizes all the parameters employed in the SCA model (some sensitivity analysis shall be carried out later). With the anisotropy ratio $f = I_v/I = 0.147$, the effective conductivity calculated by the SC approach [*Dagan*, 1989] is $K_{efh}/K_G = 3.62$, which provides a mean Eulerian velocity $U = K_{ef} J/\theta = 0.032$ m/d.

[42] The theoretical and experimental mass distributions for the six sampling rounds of the MADE-1 experiment are shown in Figure 2. The mass distributions are normalized with respect to the injected mass. The experimental curves are somewhat jagged because the data interpolation was made with the rather coarse spatial interval of 10 m [*Adams and Gelhar*, 1992]. The area below the experimental curves is not unit as it reflects the incomplete (or exceeding, for $t = 49$ days) mass recovery, which was equal to 2.06, 0.99, 0.68, 0.62, 0.54, 0.43 for $t = 49$, 126, 202, 279, 370, 503 days, respectively. In contrast, the total normalized mass of the SCA model is always unit by definition, as no retention/decay mechanisms were introduced in the model.

[43] The reservations regarding ergodicity and the initial injection conditions notwithstanding, Figures 2a–f show that the SCA model can perform satisfactorily in predicting the mass distribution of the MADE-1 experiment. We remind again that no fitting was performed, and all the data employed in the model (Table 1) are either structural or flow related, and no plume data have been used.

[44] Clearly, there is generally a difference in the tail of $m(x, t)$ due to incomplete mass recovery, and while other explanations have been advanced in previous works we tend to believe that the downstream plume truncation, as described by *Adams and Gelhar* [1992], and the insufficient density of samplers beyond a distance of about 20 m from the source may explain the "missing mass" (see the discussion of section 2). If so, the latter may be more concentrated downstream, at distances larger than those pertaining the peak of $m(x, t)$. The latter argument may explain why the SCA curve is generally above the experimental one at such distances. It is worthwhile to mention that the discrepancy is not present at $t = 126$ days, for which recovery was complete. At any rate, the location and the magnitude of

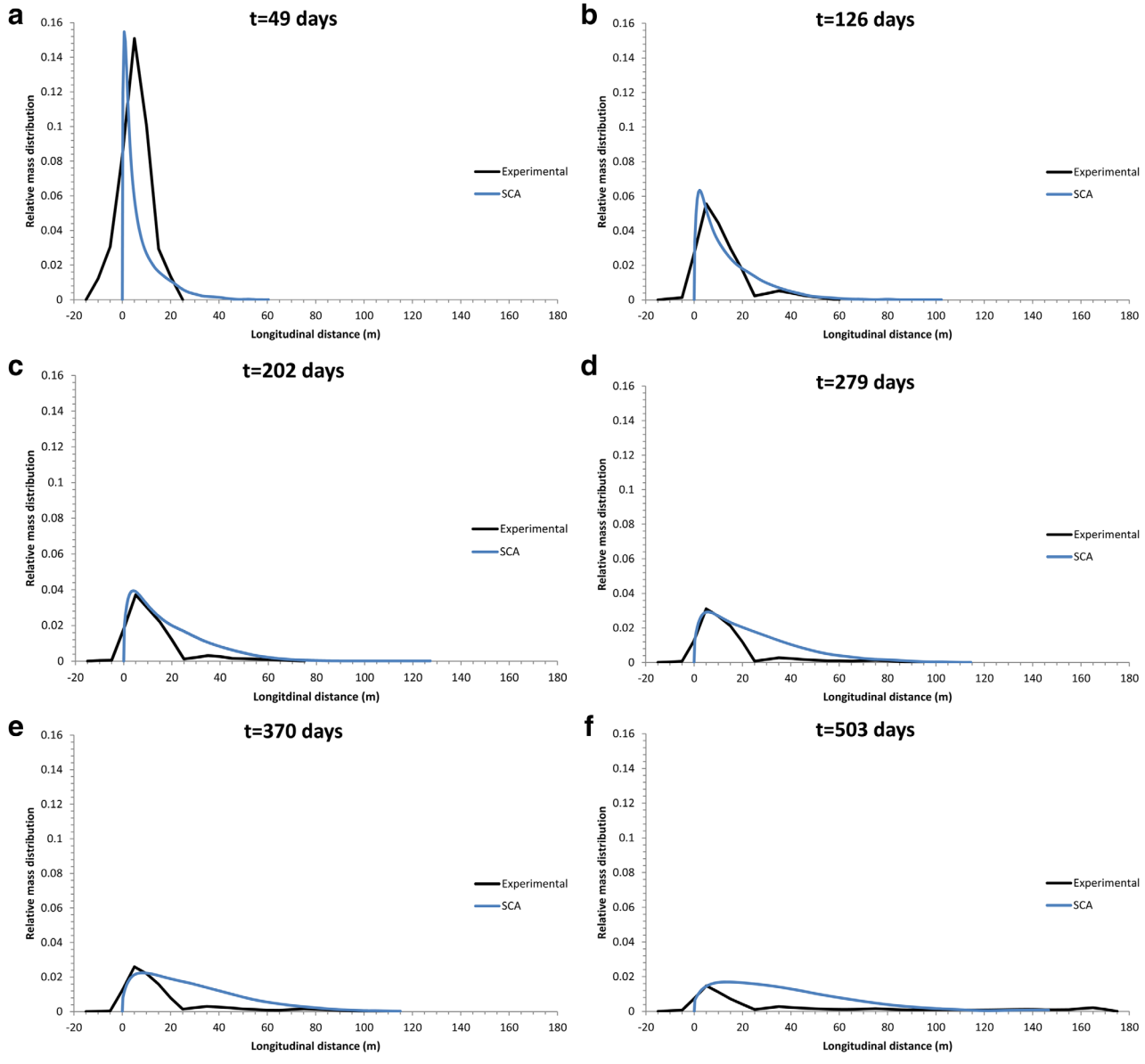

Figure 2. Longitudinal mass distribution $m(x)$ at the MADE site: experimental results (black) and theoretical prediction (SCA, blue line) for the six sampling rounds of the MADE-1 experiment [(a) to (f)].

the peak of m is captured fairly well by SCA in all cases. Comparison with the mass distribution for the MADE-2 experiment at $t = 328$ days (not shown here) confirms the results of Figure 2.

[45] We note that the spatial behavior of m displays a peak close to the injection zone and a long downstream tail. The peak reflects the long resident time spent by the solute in low-conductive regions of the aquifers, the volume fraction of which is not small because of the high heterogeneity (i.e., $\sigma_Y^2 > 1$). In turn, the long tail of m is related to the fast, preferential flow which occurs for high heterogeneity (the issue is discussed in *Fiori and Janković* [2012]). Both features are captured by SCA, which is indeed physically based, and are similar to the properties of transport sometimes denoted in literature as "anomalous". It is worthwhile to note that such anomalous features could be modeled here by a pure advection model, without invoking additional mechanisms, such e.g., retention by memory functions or partitions between mobile-immobile subdomains. In contrast, the mass distribution predicted by GADE is much more regular and symmetric, as described in the Introduction.

[46] We remind again that in any case a "perfect" agreement between theory and experiments is not possible for MADE, because of the reasons mentioned above and in section 3. Nevertheless, the predictive ability of the SCA is

Table 1. Structural Parameters Adopted in the SCA Model

$K_G = 8.9 \cdot 10^{-6}$	Geometric mean of K [m/s]
$\sigma_Y^2 = 6.6$	Logconductivity variance
$I = 10.2$	Horizontal integral scale of K [m]
$I_v = 1.5$	Vertical integral scale of K [m]
$\theta = 0.31$	Porosity
$J = 0.0036$	Mean head gradient

quite remarkable, especially considering the complete lack of calibration and use of structural parameters alone.

[47] The results of Figure 2 have been obtained by adopting the parameters of Table 1, which are based on the recent DPIL measurements [*Bohling et al.*, 2012]. As discussed in section 2, the original K statistics obtained by flowmeter [*Rehfeldt et al.*, 1992] yielded the following parameters values: $K_G = 4.3 \cdot 10^{-5}$ m/s, $I = 12.3$ m, $I_v = 1.5$ m, $\sigma_Y^2 = 4.4$. While the integral scales are similar to the DPIL ones, the variance and K_G are quite different; in particular, the geometric mean is about 5 times larger than DPIL. In turn, the measured mean gradient J exhibited smaller variations (see section 2). While σ_Y^2 influences the mechanisms embedded in SCA, K_G and J only impact the mean velocity U, and a sensitivity analysis could be performed only with regard to U and σ_Y^2. Rather than a systematic sensitivity analysis, we chose to assess the changes of prediction of m due to the above different sets of parameters. For the sake of brevity, the analysis is performed on the time instance $t = 279$ days of MADE-1; variations are similar for the other times.

[48] We analyze first variations of the mean gradient $J = 0.003$, 0.0036, 0.0042, corresponding to 20% differences from the "base" value $J = 0.003$ identified by *Adams and Gelhar* [1992]; the two extremes roughly correspond to the limits of the measured J (see section 2). Figure 3 (blue curves) displays $m(x, t)$ for the DPIL data and the three values above for J. It is seen that variations are quite small, although not negligible. Hence, variation of J (i.e., U) of the order of 20% or so do not significantly impact the mass distribution at MADE.

[49] Then, we adopted the flowmeter data reported above, resulting in a mass distribution depicted by the green curve of Figure 3. The curve based on the flowmeter data displays a significant overestimation of dispersion. This is mainly due by the much larger K_G inferred by the flowmeter, and the consequently larger U. Conversely, the impact of the lower σ_Y^2 on transport is less significant. This is illustrated by the red curve of Figure 3, which depicts the mass distribution for the DPIL data of Table 1, but with $\sigma_Y^2 = 4.4$ instead of the original $\sigma_Y^2 = 6.6$. Thus, the great disparity between the flowmeter and DPIL-based mass distribution is due to the large differences of the K_G estimates. Hence, the comparisons between experiments and SCA are fully compatible with the recent DPIL estimates of the K statistics. This finding also calls for scrutiny of previous simulations of the MADE plume based on the flowmeter data. It also constitutes an indirect validation of the DPIL technology.

5. Summary and Conclusions

[50] The relative mass distribution function $m(x,t)$ measured at MADE departs from the Gaussian shape predicted by stochastic models pertinent to weakly heterogeneous formations (first order in σ_Y^2). We have developed a model whose starting point, similarly to the first-order approximation, is the local ADE (LADE) with a spatially variable advective term. The model, which combines the MIM structure of cubes on one hand, and the SCA to solve flow and transport on the other, is conceptually, as well as computationally, simple. In essence, a parcel of solute mass moves, from the injection plane $x = 0$ to the control plane at x, past a few blocks of different K and the travel time residual is the sum of the corresponding independent steps $\tau_M(\kappa)$. The latter was derived analytically for any $\kappa = K/K_{ef}$ and the travel time pdf, which is identical to the relative solute mass flux μ (closely related to m), is determined for the lognormal pdf $f(\kappa)$ and the independent $\tau_M(\kappa)$, for any σ_Y^2. The asymmetry of m stems from that of $\tau_M(\kappa)$: the delay caused by blocks of $\kappa \ll 1$ is much larger than the advance associated with blocks of $\kappa \gg 1$. In contrast, for weak heterogeneity, i.e., κ close to unity, $\tau_M(\kappa)$ is symmetrical in $\ln \kappa$, which results in a Gaussian m.

[51] The simple model could predict in a satisfactory manner the plume mass distribution at MADE, the input information being the flow and structural parameters J, K_G, σ_Y^2, and I. The latter were inferred from the data collected in the aquifer characterization stage, independently of the transport results. Hence, local advection and the

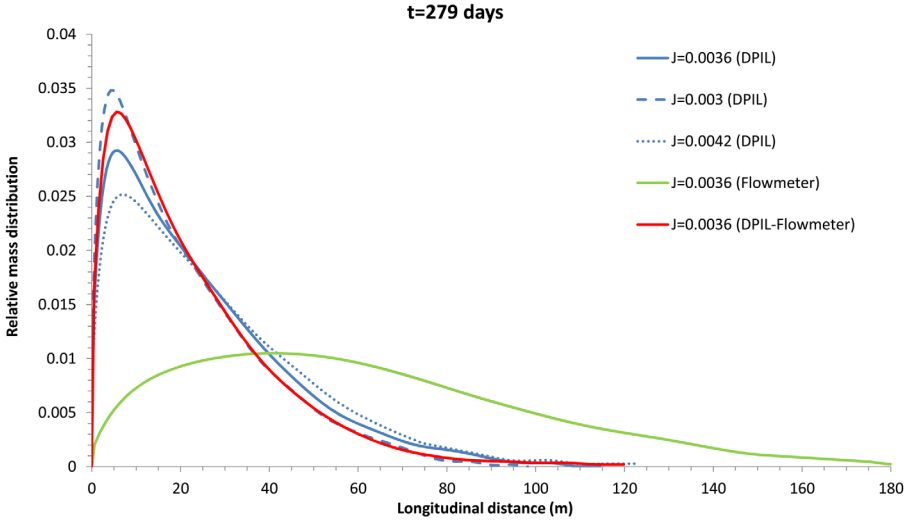

Figure 3. Changes in the mass distribution m for variations of the parameters; blue lines: DPIL data and changes in J; green line: flowmeter data; red line: DPIL data with $\sigma_Y^2 = 4.4$ (from flowmeter data).

conductivity spatial variability are apparently the only mechanisms needed in order to explain and predict the MADE findings.

[52] The present study shall be regarded as a first attempt to predict the observed MADE solute plume by using a simple model of advective transport in highly heterogeneous formations. In view of the favorable outcome, it is worthwhile to extend the scope by investigating in the future a few additional topics mentioned in section 1, like accuracy of the ergodic assumption and impact of conditioning on K data.

Appendix A: Algorithm for the Calculation of Mass Distribution along SCA

[53] The random displacement of an element of mass in the x direction is described by

$$X(t) = \sum_{i=1}^{N} l_i, \tag{A1}$$

where N is the number of blocks, of size $2I$, covered by the particle injected at $t = 0$, until time t; l_i is the length of each "step" i. The displacement (A1) is a random variable, and its pdf $f(X)$ is closely related to the mass distribution m, which is our target. After calculating K_{ef} (8), the pdf $f(X)$ is calculated by a simple Monte Carlo procedure, which closely follows the SCA model.

[54] The starting point is the travel time residual τ_R of the solute particle to cross the generic block of conductivity K is given by [*Fiori et al*., 2006]

$$\frac{\tau_R U}{R} = \frac{2}{3}(1-\kappa)\left[\frac{2}{\kappa} + \frac{3}{2+\kappa} 2F_1\left(\frac{2}{3}, 1, \frac{5}{3}, Z\right)\right]; Z = \frac{2(1-\kappa)}{(2+\kappa)}, \tag{A2}$$

where ${}_2F_1$ is the hypergeometric function, given by

$${}_2F_1\left(\frac{2}{3}, 1, \frac{5}{3}, Z\right) = \frac{1}{3\zeta^2}\begin{cases} \ln\left[\dfrac{1+\zeta+\zeta^2}{(1-\zeta)^2}\right] - 2\sqrt{3}\arctan\left(\dfrac{\sqrt{3}\zeta}{\zeta+2}\right) (1 \geq \kappa \geq 0 \rightarrow 0 \leq Z \leq 1) \\ \ln\left[\dfrac{1-\zeta+\zeta^2}{(1+\zeta)^2}\right] - 2\sqrt{3}\arctan\left(\dfrac{\sqrt{3}\zeta}{\zeta-2}\right) (\infty \geq \kappa \geq 1 \rightarrow -2 \leq Z \leq 0) \end{cases}, \tag{A3}$$

with $\kappa = K/K_{ef}$ and $\zeta = |Z|^{1/3}$. The particle trajectory X is calculated along the following procedure.

[55] 1. Since the location of the initial plume with respect the planes separating blocks is an artifact of the representation of the structure (Figure 1a), the first step l_1 is regarded as a random variable of uniform distribution between 0 and $2I$, while the other steps are of length $2I$; then, the conductivity K_1 is randomly generated, which provides the interior velocity $V_{in,1} = 3\kappa_1/(2+\kappa_1)$, with $\kappa_1 = K_1/K_{ef}$, and the travel time residual $\tau_{R,1}$ (A2) for the first block; since the first step is generally smaller than $2I$, the travel time within the first block is scaled down by the factor $\phi = \ell_1/(2I)$. The mass attached to the particle is proportional to V_{in1} / U.

[56] 2. The particle travel time pertaining to the block $i = 1$ is $\ell_1/U + \phi(\tau_{R,1} - \delta)$. Here $\delta = \int V_{in}(\kappa)\tau_R(\kappa)f(\kappa)\mathrm{d}\kappa$ stands for a drift which takes into account the neglect of transport on streamlines outside the wake (for further details, see *Fiori et al*. [2006]); it has to be computed only once. Next, if $\ell_1/U + \phi(\tau_{R,1} - \delta) < t$, the particle moves into the second block, of conductivity K_2; the latter is again randomly generated, providing $V_{in,2}, \tau_{R,2}$. Another check is carried out to determine if $\ell_1/U + \phi\tau_{R1} + 2I_Y/U + \tau_{R2} - (1+\phi)\delta < t$, in which case the particle moves to the next block of conductivity K_3, and the above procedure is repeated.

[57] 3. The procedure stops when $\sum_{i=1}^{N}(\tau_R(l_i, K_i) + l_i/U - \delta) \geq t$. In such case, the last step l_N is scaled down by the same factor ϕ previously illustrated, such that the condition $\sum_{i=1}^{N}(\tau_R(l_i, K_i) + l_i/U - \delta) = t$ is fully satisfied. Thus, the particle displacement and its mass are given by $X(t) = \sum_{i=1}^{N} l_i$ and $\Delta = \Pi_{i=1}^{N} V_{in,i}/U$, respectively.

[58] 4. The entire procedure 1–3 is repeated M times, leading to the generation of M independent particles, each one with its own displacement X and mass Δ. The plume mass distribution $m(x,t)$ is determined subsequently through a simple frequency distribution applied to the M values of $X(t)$.

[59] The code built along these lines, by a Monte Carlo procedure, is very simple and fast. For the MADE implementation, we employed $M = 200{,}000$ and the run for a given t typically takes a few minutes on a regular PC. Since the model is ergodic, the full K distribution is sampled and no conditioning is made on data.

[60] **Acknowledgments.** Support for the project "Innovative Methods for Water Resources Management Under Hydro-Climatic Uncertainty Scenarios" (2010JHF437) funded by the Italian Ministry of Education is acknowledged.

References

Adams, E.E., and L.W. Gelhar (1992), Field study of dispersion in a heterogeneous aquifer: 2. Spatial moments analysis, *Water Resour. Res.*, *28*(12), 3293–3307, doi:10.1029/92WR01757.

Bear, J. (1988), *Dynamics of Fluids in Porous Media*, 764 pp., Dover, New York.

Berglund, S., and A. Fiori (1997), Influence of transverse mixing on the breakthrough of sorbing solute in a heterogeneous aquifer, *Water Resour. Res.*, *33*(3), 399–405, doi:10.1029/96WR03686.

Berkowitz, B., and H. Scher (1998), Theory of anomalous chemical transport in random fracture networks, *Phys. Rev. E*, *57*(5), 5858–5869.

Boggs, J.M., and E.E. Adams (1992), Field study of dispersion in a heterogeneous aquifer: 4. Investigation of adsorption and sampling bias, *Water Resour. Res.*, *28*(12), 3325–3336, doi:10.1029/92WR01759.

Boggs, J.M., S.C. Young, L.M. Beard, L.W. Gelhar, K.R. Rehfeldt, and E.E. Adams (1992), Field study of dispersion in a heterogeneous aquifer:

1. Overview and site description, *Water Resour. Res.*, *28*(12), 3281–3291, doi:10.1029/92WR01756.

Boggs, J.M., L.M. Beard, S.E. Long, M.P. McGee, W.G. MacIntyre, C.P. Antworth, and T.B. Stauffer (1993), Database for the second macrodispersion experiment (MADE-2), *Tech. Rep. TR-102072*, Electr. Power Res. Inst., Palo Alto, Calif.

Bohling, G.C., G. Liu, S.J. Knobbe, E.C. Reboulet, D.W. Hyndman, P. Dietrich, and J.J. Butler Jr. (2012), Geostatistical analysis of centimeter-scale hydraulic conductivity variations at the MADE site, *Water Resour. Res.*, *48*, W02525, doi:10.1029/2011WR010791.

Dagan, G. (1979), Models of groundwater flow in statistically homogeneous porous formations, *Water Resour. Res.*, *15*(1), 47–63, doi:10.1029/WR015i001p00047.

Dagan, G. (1989), *Flow and Transport in Porous Formations*, Springer, New York.

Dagan, G., A. Fiori, and I. Janković (2003), Flow and transport in highly heterogeneous formations: 1. Conceptual framework and validity of first-order approximations, *Water Resour. Res.*, *39*(9), 1268, doi:10.1029/2002WR001717.

Dagan, G., A. Fiori, and I. Jankovic (2008), *Transport in porous media, in Encyclopedia of Ecology*, edited by S.E. Jorgensen and B.D. Fath, pp. 3576–3582, Oxford, Elsevier.

de Dreuzy, J.-R., A. Beaudoin, and J. Erhel (2007), Asymptotic dispersion in 2D heterogeneous porous media determined by parallel numerical simulations, *Water Resour. Res.*, *43*, W10439, doi:10.1029/2006WR005394.

Eames, I., and J.W. Bush (1999), Longitudinal dispersion by bodies fixed in a potential flow, *Proc. R. Soc. London, Ser. A.*, *455*, 3665–3686, doi:10.1098/rspa.1999.0471.

Feehley, C.E., C. Zheng, and F.J. Molz (2000), A dual-domain mass transfer approach for modeling solute transport in heterogeneous aquifers: Application to the macrodispersion experiment (MADE) site, *Water Resour. Res.*, *36*(9), 2501–2515, doi:10.1029/2000WR900148.

Fiori, A. (1996), Finite Peclet extensions of Dagan's solutions to transport in anisotropic heterogeneous formations, *Water Resour. Res.*, *32*(1), 193–198, doi:10.1029/95WR02768.

Fiori, A., and I. Janković (2012), On preferential flow, channeling and connectivity in heterogeneous porous formations, *Math. Geosci.*, *44*, 133–145, doi:10.1007/s11004-011-9365-2.

Fiori, A., I. Janković, and G. Dagan (2003), Flow and transport in highly heterogeneous formations: 2. Semianalytical results for isotropic media, *Water Resour. Res.*, *39*(9), 1269, doi:10.1029/2002WR001719.

Fiori, A., I. Janković, and G. Dagan (2006), Modeling flow and transport in highly heterogeneous three-dimensional aquifers: Ergodicity, Gaussianity, and anomalous behavior—2. Approximate semianalytical solution, *Water Resour. Res.*, *42*, W06D13, doi:10.1029/2005WR004752.

Fiori, A., I. Janković, G. Dagan, and V. Cvetković (2007), Ergodic transport through aquifers of non-Gaussian log conductivity distribution and occurrence of anomalous behavior, *Water Resour. Res.*, *43*, W09407, doi:10.1029/2007WR005976.

Fiori, A., G. Dagan, and I. Janković (2012), Comment on "Comparison of Fickian and temporally nonlocal transport theories over many scales in an exhaustively sampled sandstone slab" by Major et al, WRR, 47, W10519, 2011, *Water Resour. Res.*, *48*, W07801, doi:10.1029/2011WR011706.

Freyberg, D.L. (1986), A natural gradient experiment on solute transport in a sand aquifer: 2. Spatial moments and the advection and dispersion of nonreactive tracers, *Water Resour. Res.*, *22*(13), 2031–2046, doi:10.1029/WR022i013p02031.

Frippiat, C.C., and A.E. Holeyman (2008), A comparative review of upscaling methods for solute transport in heterogeneous porous media, *J. Hydrol.*, *362*(1–2), 150–176, doi:10.1016/j.jhydrol.2008.08.015.

Garabedian, S.P., D.R. LeBlanc, L.W. Gelhar, and M.A. Celia (1991), Large-scale natural gradient tracer test in sand and gravel, Cape Cod, Massachusetts: 2. Analysis of spatial moments for a nonreactive tracer, *Water Resour. Res.*, *27*(5), 911–924, doi:10.1029/91WR00242.

Gelhar, L.W. (1993), *Stochastic Subsurface Hydrology*, 390 pp., Prentice-Hall, Upper Saddle River, N.Y.

Gelhar, L.W., and C.L. Axness (1983), Three-dimensional stochastic analysis of macrodispersion in aquifers, *Water Resour. Res.*, *19*(1), 161–180, doi:10.1029/WR019i001p00161.

Guan, J., F.J. Molz, Q. Zhou, H.H. Liu, and C. Zheng (2008), Behavior of the mass transfer coefficient during the MADE-2 experiment: New insights, *Water Resour. Res.*, *44*, W02423, doi:10.1029/2007WR006120.

Harvey, C. and S.M. Gorelick (2000), Rate-limited mass transfer or macrodispersion: Which dominates plume evolution at the macrodispersion experiment (MADE) site? *Water Resour. Res.*, *36*(3), 637–650, doi:10.1029/1999WR900247.

Janković, I., and A. Fiori (2010), Analysis of the impact of injection mode in transport through strongly heterogeneous aquifers, *Adv. Water Resour.*, *33*, 1199–1205, doi:10.1016/j.advwatres.2010.05.006.

Janković, I., A. Fiori, and G. Dagan (2003), Flow and transport in highly heterogeneous formations: 3. Numerical simulations and comparison with theoretical results, *Water Resour. Res.*, *39*(9), 1270, doi:10.1029/2002WR001721.

Janković, I., A. Fiori, and G. Dagan (2006), Modeling flow and transport in highly heterogeneous three-dimensional aquifers: Ergodicity, Gaussianity, and anomalous behavior—1. Conceptual issues and numerical simulations, *Water Resour. Res.*, *42*, W06D12, doi:10.1029/2005WR004734.

Janković, I., A. Fiori, and G. Dagan (2009), The impact of local diffusion on longitudinal macrodispersivity and its major effect upon anomalous transport in highly heterogeneous aquifers, *Adv. Water Resour.*, *32*(5), 659–669, doi:10.1016/j.advwatres.2008.08.012.

Janković I., Fiori A., and Dagan G. (2013), Effective conductivity of isotropic highly heterogeneous formations: Numerical and theoretical issues, *Water Resour. Res.*, *49*, doi:10.1029/2012WR012441.

LeBlanc, D.R., S.P. Garabedian, K.M. Hess, L.W. Gelhar, R.D. Quadri, K.G. Stollenwerk, and W.W. Wood (1991), Large-scale natural gradient tracer test in sand and gravel, Cape Cod, Massachusetts: 1. Experimental design and observed tracer movement, *Water Resour. Res.*, *27*(5), 895–910, doi:10.1029/91WR00241.

Liu, G., J.J. Butler Jr., G.C. Bohling, E. Reboulet, S. Knobbe and D.W. Hyndman (2009), A new method for high-resolution characterization of hydraulic conductivity, *Water Resour. Res.*, *45*, W08202, doi:10.1029/2009WR008319.

Mackay, D.M., D.L. Freyberg, P.V. Roberts, and J.A. Cherry (1986), A natural gradient experiment on solute transport in a sand aquifer: 1. Approach and overview of plume movement, *Water Resour. Res.*, *22*(13), 2017–2029, doi:10.1029/WR022i013p02017.

Major, E., D.A. Benson, J. Revielle, H. Ibrahim, A. Dean, R.M. Maxwell, E. Poeter, and M. Dogan (2011), Comparison of Fickian and temporally nonlocal transport theories over many scales in an exhaustively sampled sandstone slab, *Water Resour. Res.*, *47*, W10519, doi:10.1029/2011WR010857.

Rajaram, H., and L.W. Gelhar (1991), Three-dimensional spatial moments analysis of the Borden Tracer Test, *Water Resour. Res.*, *27*(6), 1239–1251, doi:10.1029/91WR00326.

Rehfeldt, K.R., J.M. Boggs, and L.W. Gelhar (1992), Field study of dispersion in a heterogeneous aquifer: 3. Geostatistical analysis of hydraulic conductivity, *Water Resour. Res.*, *28*(12), 3309–3324, doi:10.1029/92WR01758.

Rubin, Y. (2003), *Applied Stochastic Hydrology*, 391 pp., Oxford Univ. Press, New York.

Salamon, P., D. Fernandez-Garcia, and J.J. Gomez-Hernandez (2007), Modeling tracer transport at the MADE site: The importance of heterogeneity, *Water Resour. Res.*, *43*, W08404, doi:10.1029/2006WR005522.

Sudicky, E.A. (1986), A natural gradient experiment on solute transport in a sand aquifer: Spatial variability of hydraulic conductivity and its role in the dispersion process, *Water Resour. Res.*, *22*(13), 2069–2082, doi:10.1029/WR022i013p02069.

Suribhatla, R., I. Janković, A. Fiori, A. Zarlenga, and G. Dagan (2011), Effective conductivity of an anisotropic heterogeneous medium of random conductivity distribution, *Multiscale Model. Simul.*, *9*(3), 933–954, doi: 10.1137/100805662.

Zarlenga, A., A. Fiori, C. Soffia, and I. Janković (2012a), Flow velocity statistics for uniform flow through 3D anisotropic formations, *Adv. Water Resour.*, *40*, 37–45, doi:10.1016/j.advwatres.2012.01.011.

Zarlenga, A., I. Janković, and A. Fiori (2012b), Advective transport in heterogeneous formations: The impact of spatial anisotropy on the Breakthrough curve. *Transp. Porous Media*, *96*(2), 295–304. doi:10.1007/s11242-012-0088-8.

Zheng, C., M. Bianchi, and S.M. Gorelick (2011), Lessons learned from 25 years of research at the MADE site, *Ground Water*, *49*, 649–662. doi:10.1111/j.1745–6584.2010.00753.x.